



HAL
open science

Targeted intestinal tight junction hyperpermeability alters the microbiome, behavior, and visceromotor responses

Orsolya Inczeffi, Valérie Alquier-Bacquié, Maïwenn Olier, Marion Rincel, B elinda Ringot-Destrez, Sandrine Ellero-Simatos, H el ene Eutam ene, Colette B etouli eres, Julie Thomas, Justin Laine, et al.

► To cite this version:

Orsolya Inczeffi, Val erie Alquier-Bacqui e, Ma iwenn Olier, Marion Rincel, B elinda Ringot-Destrez, et al.. Targeted intestinal tight junction hyperpermeability alters the microbiome, behavior, and visceromotor responses. *Cellular and Molecular Gastroenterology and Hepatology*, 2020, 10 (1), pp.1-6. 10.1016/j.jcmgh.2020.02.008 . hal-02624659

HAL Id: hal-02624659

<https://hal.inrae.fr/hal-02624659>

Submitted on 26 May 2020

HAL is a multi-disciplinary open access archive for the deposit and dissemination of scientific research documents, whether they are published or not. The documents may come from teaching and research institutions in France or abroad, or from public or private research centers.

L'archive ouverte pluridisciplinaire **HAL**, est destin ee au d ep ot et  a la diffusion de documents scientifiques de niveau recherche, publi es ou non,  emanant des  tablissements d'enseignement et de recherche fran ais ou  trangers, des laboratoires publics ou priv es.



Distributed under a Creative Commons Attribution - NonCommercial - NoDerivatives 4.0 International License

Journal Pre-proof



Targeted intestinal tight junction hyperpermeability alters the microbiome, behavior, and visceromotor responses

Orsolya Inczeffi, Valérie Bacquié, Maiwenn Olier-Pierre, Marion Rincel, Belinda Ringot-Destrez, Sandrine Ellero-Simatos, Hélène Eutamène, Colette Bétoulières, Julie Thomas, Justin Laine, Louise Gros, Mathilde Lévêque, Renaud Leonard, Cheryl Harkat, Catherine Robbe-Masselot, Richard Roka, Muriel Mercier-Bonin, Vassilia Theodorou, Muriel Darnaudéry, Jerrold R. Turner, Laurent Ferrier

PII: S2352-345X(20)30035-7
DOI: <https://doi.org/10.1016/j.jcmgh.2020.02.008>
Reference: JCMGH 588

To appear in: *Cellular and Molecular Gastroenterology and Hepatology*
Accepted Date: 27 February 2020

Please cite this article as: Inczeffi O, Bacquié V, Olier-Pierre M, Rincel M, Ringot-Destrez B, Ellero-Simatos S, Eutamène H, Bétoulières C, Thomas J, Laine J, Gros L, Lévêque M, Leonard R, Harkat C, Robbe-Masselot C, Roka R, Mercier-Bonin M, Theodorou V, Darnaudéry M, Turner JR, Ferrier L, Targeted intestinal tight junction hyperpermeability alters the microbiome, behavior, and visceromotor responses, *Cellular and Molecular Gastroenterology and Hepatology* (2020), doi: <https://doi.org/10.1016/j.jcmgh.2020.02.008>.

This is a PDF file of an article that has undergone enhancements after acceptance, such as the addition of a cover page and metadata, and formatting for readability, but it is not yet the definitive version of record. This version will undergo additional copyediting, typesetting and review before it is published in its final form, but we are providing this version to give early visibility of the article. Please note that, during the production process, errors may be discovered which could affect the content, and all legal disclaimers that apply to the journal pertain.

© 2020 The Authors. Published by Elsevier Inc. on behalf of the AGA Institute.

Comment citer ce document :

Inczeffi, O., Bacquié, V., Olier Pierre, M., Rincel, M., Ringot-Destrez, B., Ellero Simatos, S., Eutamene, H., Bétoulières, C., Thomas, J., Laine, J., Gross, L., Lévêque, M., Leonard, Harkat, C., Robbe-Masselot, Roka, R., Mercier-Bonin, M., Theodorou, V., Darnaudéry, M., Turner, J. R., Ferrier, L. (Auteur de correspondance) (2020). Targeted intestinal tight junction

Targeted intestinal tight junction hyperpermeability alters the microbiome, behavior, and visceromotor responses

Orsolya Inczefi^{1,2,*}, Valérie Bacquié^{1,*}, Maïwenn Olier-Pierre¹, Marion Rincel³, Belinda Ringot-Destrez⁴, Sandrine Ellero-Simatos¹, Hélène Eutamène¹, Colette Bétoulières¹, Julie Thomas³, Justin Laine³, Louise Gros³, Mathilde Lévêque¹, Renaud Leonard⁴, Cherryl Harkat¹, Catherine Robbe-Masselot⁴, Richard Roka², Muriel Mercier-Bonin¹, Vassilia Theodorou¹, Muriel Darnaudéry³, Jerrold R Turner^{5§}, and Laurent Ferrier^{1§}

¹ INRAE, UMR 1331 ToxAlim, Toulouse, France

² First Department of Medicine, University of Szeged, Szeged, Hungary

³ University of Bordeaux, INRAE, Nutrition and Integrative Neurobiology, UMR 1286, 33076 Bordeaux, France

⁴ Université de Lille, Unité de Glycobiologie Structurale et Fonctionnelle, Villeneuve d'Ascq, France

⁵ Laboratory of Mucosal Barrier Pathobiology, Department of Pathology, Brigham and Women's Hospital, Harvard Medical School, Boston, Massachusetts, USA

* These authors contributed equally

§Corresponding authors:

Laurent Ferrier, PhD

INRA, UMR 1331 ToxAlim, Group of Neuro-Gastroenterology & Nutrition, Toulouse, France

Present address: Nestlé Research, Institute of Health Sciences, Department of Gastro-Intestinal Health

Route du Jorat 57 – Vers-chez-les-Blanc

1000 Lausanne 26

Switzerland

Phone: +41 21 785 84 21

E-mail: laurent.ferrier@rd.nestle.com

Jerrold R. Turner, MD, PhD

77 Avenue Louis Pasteur

NRB 730

Boston, MA 02115

E-mail: jrturner@bwh.harvard.edu

LENGTH: 999 words

RUNNING HEADER: Diverse responses to intestinal hyperpermeability

CONFLICTS OF INTEREST: JRT is a cofounder of Thelium Therapeutics. LF is currently an employee of Nestlé Research (Société des Produits Nestlé S.A.).

CONTRIBUTIONS: Conceptualization: MOP, MMB, MD, VT, JRT, LF; Experimentation: OI, VB, MOP, BRD, MR, SES, CB, ML, JT, JL, LG, RL, CH; Data analysis: OI, VB, MOP, HE, CRM, MR, RR, MMB, MD, JRT, LF; Manuscript preparation and revision: MD, JRT, LF.

KEYWORDS: myosin light chain kinase, MLCK, tight junction, microbiome, stress

ACKNOWLEDGEMENTS: This work was supported by an institutional grant from INRA and by NIH grants R01DK61931 and R01DK68271 to JRT. MD was supported by Bordeaux University, by the FFAS (Fond Français Alimentation Santé), and the ANR (Agence Nationale de la Recherche). MR was supported by the French ministry of research and education and Labex Brain. JT was a recipient of a fellowship from the French Society of Paediatric Research. OI was a recipient of a fellowship from the Nutrition, Chemical Food Safety and Consumer Behaviour Division of INRA.

Comment citer ce document :

Inczefi, O., Bacquié, V., Olier Pierre, M., Rincel, M., Ringot-Destrez, B., Ellero Simatos, S., Eutamene, H., Bétoulières, C., Thomas, J., Laine, J., Gross, L., Lévêque, M., Leonard, Harkat, C., Robbe-Masselot, Roka, R., Mercier-Bonin, M., Theodorou, V., Darnaudéry, M., Turner, J. R., Ferrier, L. (Auteur de correspondance) (2020). Targeted intestinal tight junction

1 Markedly increased intestinal permeability occurs in inflammatory bowel disease (IBD), graft-
2 versus-host disease (GVHD), celiac disease, and multiple organ dysfunction. In these
3 diseases, effectors of increased permeability include immune signaling,¹ microbiome,² and
4 corticosteroids³ that, in part, signal through epithelial myosin light chain kinase (MLCK). More
5 modest permeability increases occur in other disorders, including irritable bowel syndrome
6 (IBS), autism spectrum disorder (ASD), depression, and stress-related disorders. Data directly
7 linking barrier loss to disease phenotypes, however, are lacking.

8 To define the impact of modestly-increased intestinal permeability, we studied transgenic mice
9 with intestinal epithelial-specific constitutively-active myosin light chain kinase (CAMLCK)
10 expression. This MLCK-dependent tight junction regulation increased intestinal permeability
11 (Fig. S1A,B).¹ Nevertheless, postnatal growth (Fig. S1C), reproduction, intestinal transit (Fig.
12 S1D), and intestinal histology, epithelial proliferation (a sensitive indicator of epithelial damage),
13 and epithelial turnover are unaffected in CAMLCK transgenic (*CAMLCK^{Tg}*) mice.¹ In contrast,
14 mucosal tumor necrosis factor- α , interferon- γ , IL-10, and IL-13 transcripts as well as numbers of
15 lamina propria neutrophils, CD4⁺ T cells, and IgA⁺ plasma cells are modestly increased by
16 CAMLCK expression.^{1,2} Subclinical inflammation is, therefore, present and, by microbiome-
17 dependent, IL-17-mediated processes, affords partial protection from acute pathogen invasion.²
18 Immune activation is nevertheless unlikely to amplify CAMLCK-driven permeability increases,
19 as barrier function and ZO-1 anchoring are both acutely normalized by enzymatic MLCK
20 inhibition.^{1,4}

21 We initially analyzed the gut microbiome of 31 WT and *CAMLCK^{Tg}* pups born to 8 WT dams.
22 The microbiomes segregated by pup genotype but not dam (Fig. S1E) and included increased
23 *Clostridium* and decreased Bacteroidetes, *Enterococcus spp*, and *Prevotella* in *CAMLCK^{Tg}* mice
24 (Fig. S1F). Increased intestinal permeability can therefore cause dysbiosis-like microbiome
25 shifts. Interestingly, maternal separation, which increases intestinal permeability, causes similar
26 alterations and can be partially corrected by MLCK inhibitor-induced barrier restoration.⁵

27 Microbiome alterations overlapping with the above have been reported in IBS and ASD. We
28 therefore asked if *CAMLCK^{Tg}* mice displayed anxiety-like behavior, as occurs in those disorders,
29 using the open-field test (Fig. 1C). Both the percentage of distance traveled in the center and
30 the fraction of time spent in the center of the open field were reduced in *CAMLCK^{Tg}* mice (Fig.
31 1C); this did not reflect reduced locomotor activity, as total distance traveled in the entire area
32 was similar in *CAMLCK^{Tg}* and WT mice (Fig. 1C). These data are consistent with increased
33 anxiety-like behavior in *CAMLCK^{Tg}* mice. Although the results cannot differentiate between

34 direct effects of increased permeability and those requiring intermediate mediators, these data
35 demonstrate that intestinal permeability increases can influence behavior.

36 Stress and increased permeability have been associated with enhanced visceral sensitivity in
37 humans and rodents. Surprisingly, *CAMLCK^{Tg}* mice displayed striking visceral analgesia to
38 colorectal distension relative to WT littermates (Fig. 1D). Sensitivity was restored by enzymatic
39 MLCK inhibition, water avoidance stress, or naloxone-mediated opioid receptor antagonism
40 (Fig. 1D). Although this effect of increased permeability on visceral sensitivity was unexpected,
41 it is remarkably similar to the naloxone-reversible visceral analgesia reported in chronically-
42 stressed female rats⁶ and naloxone-sensitive inhibition of nociceptive neurons by supernatants
43 of colitic human and murine tissues.⁷

44 Studies of female IBS patients have linked increased permeability to altered functional and
45 structural brain connectivity.⁸ Thus, although responses to colorectal distension can be
46 mediated by spinal reflexes and sensory, limbic, and paralimbic regions of the brain,⁹ we asked
47 if neuronal activation was modified by *CAMLCK*-induced permeability increases. C-Fos
48 immunolabeling, an indicator of neuronal activity, was significantly greater in the paraventricular
49 nucleus of the thalamus, the paraventricular nucleus of the hypothalamus, and the
50 hippocampus, but not the medial prefrontal cortex, nucleus accumbens, or amygdala, of
51 *CAMLCK^{Tg}*, relative to WT, mice (Figs. 2, S2). Increased intestinal permeability may therefore
52 increase basal neuronal activity in areas of the brain that regulate responses to visceral pain or
53 stress⁹ but not those associated with conscious visceral sensation.

54 These results demonstrate that increased intestinal permeability can impact i) gut microbiome
55 composition; ii) behavior; iii) visceral pain responses; and iv) neuronal activation within the
56 brain. Critically, these changes are all results, rather than causes, of intestinal barrier loss, as
57 the latter was induced by targeted *CAMLCK* expression.

58 The sites of neuronal activation in *CAMLCK^{Tg}* mice support the hypothesis that increased
59 intestinal permeability can activate the hypothalamic-pituitary-adrenal axis.¹⁰ Conversely,
60 hypothalamic-pituitary-adrenal axis activation by exogenous stress can induce intestinal
61 permeability increases.³ Thus, as has been proposed in IBD and GVHD, a self-amplifying cycle
62 may ultimately direct the diverse phenotypes induced by MLCK-dependent, intestinal
63 permeability increases. Further study is needed to define the complex relationships between
64 intestinal permeability, stress, behavioral alterations, visceromotor responses, microbiome
65 composition, and other abnormalities.

66 These data are the first to assess behavior in a model where a targeted increase in intestinal
67 tight junction permeability is the only direct perturbation. The results demonstrate,
68 unequivocally, that modest tight junction permeability increases induced via a physiologically-
69 and pathophysiologically-relevant mechanism are sufficient to trigger local and systemic
70 microbial, behavioral, and neurosensory changes. This provides new perspective with which to
71 understand previously hypothesized cause-effect relationships that have been proposed on the
72 basis of correlative data.

73

Journal Pre-proof

Comment citer ce document :

Inczefi, O., Bacquié, V., Olier Pierre, M., Rincel, M., Ringot-Destrez, B., Ellero Simatos, S., Eutamene, H., Bétoulières, C., Thomas, J., Laine, J., Gross, L., Lévêque, M., Leonard, Harkat, C., Robbe-Masselot, Roka, R., Mercier-Bonin, M., Theodorou, V., Darnaudéry, M., Turner, J. R., Ferrier, L. (Auteur de correspondance) (2020). Targeted intestinal tight junction

74 **Figure legends:**

75 **Figure 1: Increased intestinal permeability modifies behavior and visceral sensitivity. A.**

76 Videotracking paths of representative WT and *CAMLCK^{Tg}* mice in the open field test. Percent
77 distance traveled in the center (dashed lines), percent time in the center, and overall distance
78 traveled in the entire field are shown. *CAMLCK^{Tg}* (blue circles, n=8) and WT (red squares, n=9)
79 littermates were tested. mean±SEM. *, $p<0.05$; **, $p<0.01$, Mann-Whitney U test. **B.** Stepwise
80 colorectal distension-induced visceromotor responses in *CAMLCK^{Tg}* (blue circles, n=7) were
81 reduced relative to WT (red squares, n=7) littermates. Genotype-specific differences were
82 eliminated by MLCK inhibition, water avoidance stress, or naloxone treatment. n = 5-9 per
83 condition; for each treatment (vehicle control *CAMLCK^{Tg}* and WT mice from the same
84 experiment are shown with pale symbols in the last three graphs). mean±SEM; **, $p<0.01$, 2-
85 way ANOVA.

86 **Figure 2: Increased intestinal permeability induces increased C-Fos immunolabelling in**

87 **selected brain regions.** *CAMLCK^{Tg}* (blue circles, n=5-6) and WT (red squares, n=5-6)
88 littermates. Representative images of C-Fos immunolabeled brains from *CAMLCK^{Tg}* and WT
89 mice. Bars = 200 μm ; mean±SEM; *, $p<0.05$, t-test.

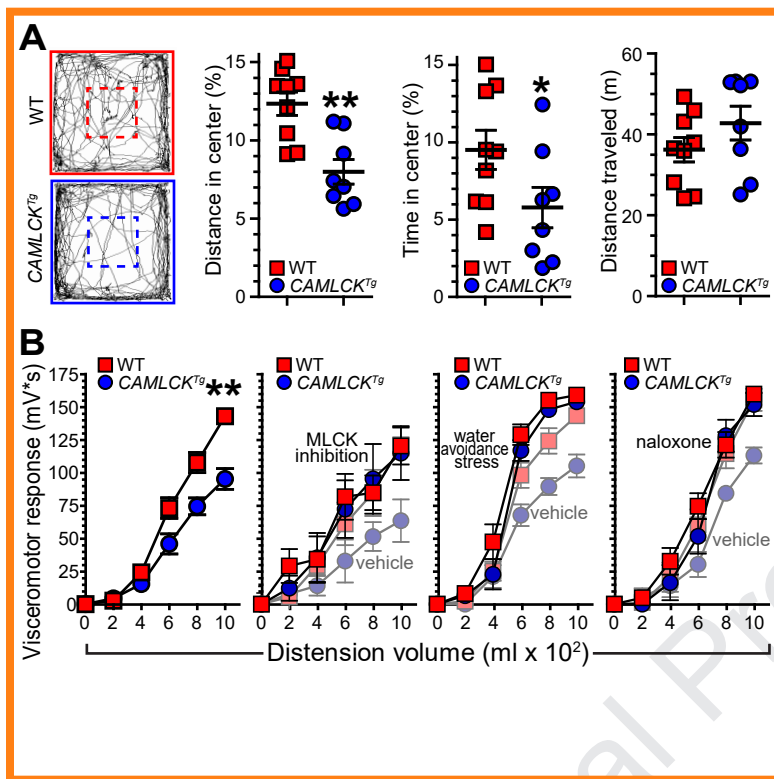
90 **References**

- 91 1. Su L, et al. *Gastroenterology* 2009;136:551-63.
- 92 2. Edelblum KL, et al. *Cell Mol Gastroenterol Hepatol* 2017;4:285-297.
- 93 3. Meddings JB, et al. *Gastroenterology* 2000;119:1019-28.
- 94 4. Yu D, et al. *Proc Natl Acad Sci U S A* 2010;107:8237-41.
- 95 5. Rincel M, et al. *Psychopharmacology (Berl)* 2019;236:1583-1596.
- 96 6. Larauche M, et al. *Neurogastroenterol Motil* 2012;24:1031-e547.
- 97 7. Guerrero-Alba R, et al. *Gut* 2017;66:2121-2131.
- 98 8. Witt ST, et al. *Neuroimage Clin* 2019;21:101602.
- 99 9. Larauche M, et al. *Neurogastroenterol Motil* 2019;31:e13489.
- 100 10. Ait-Belgnaoui A, et al. *Psychoneuroendocrinology* 2012;37:1885-95.

101

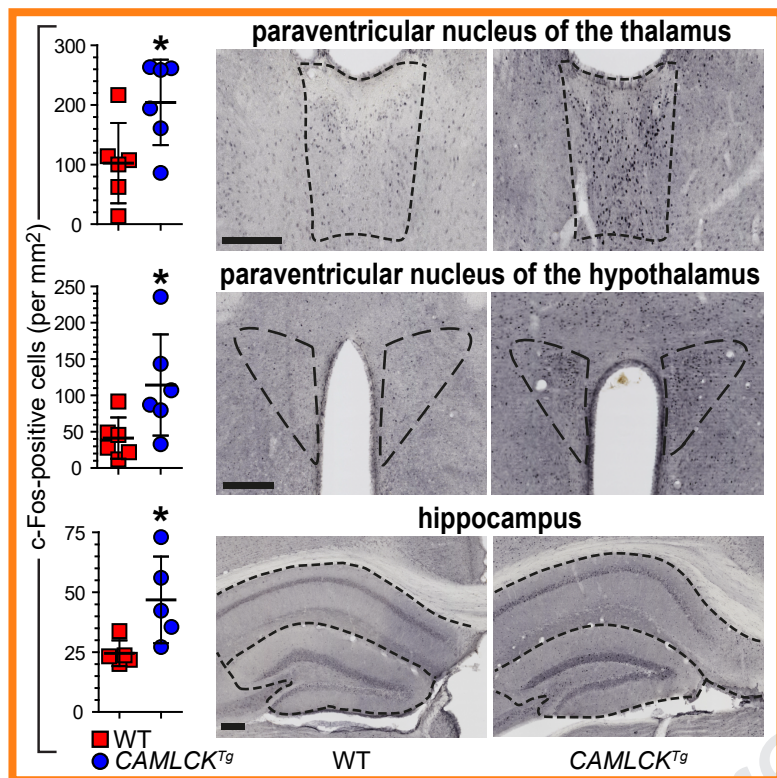
Comment citer ce document :

Inczefi, O., Bacquié, V., Olier Pierre, M., Rincel, M., Ringot-Destrez, B., Ellero Simatos, S., Eutamene, H., Bétoulières, C., Thomas, J., Laine, J., Gross, L., Lévêque, M., Leonard, Harkat, C., Robbe-Masselot, Roka, R., Mercier-Bonin, M., Theodorou, V., Darnaudéry, M., Turner, J. R., Ferrier, L. (Auteur de correspondance) (2020). Targeted intestinal tight junction



Comment citer ce document :

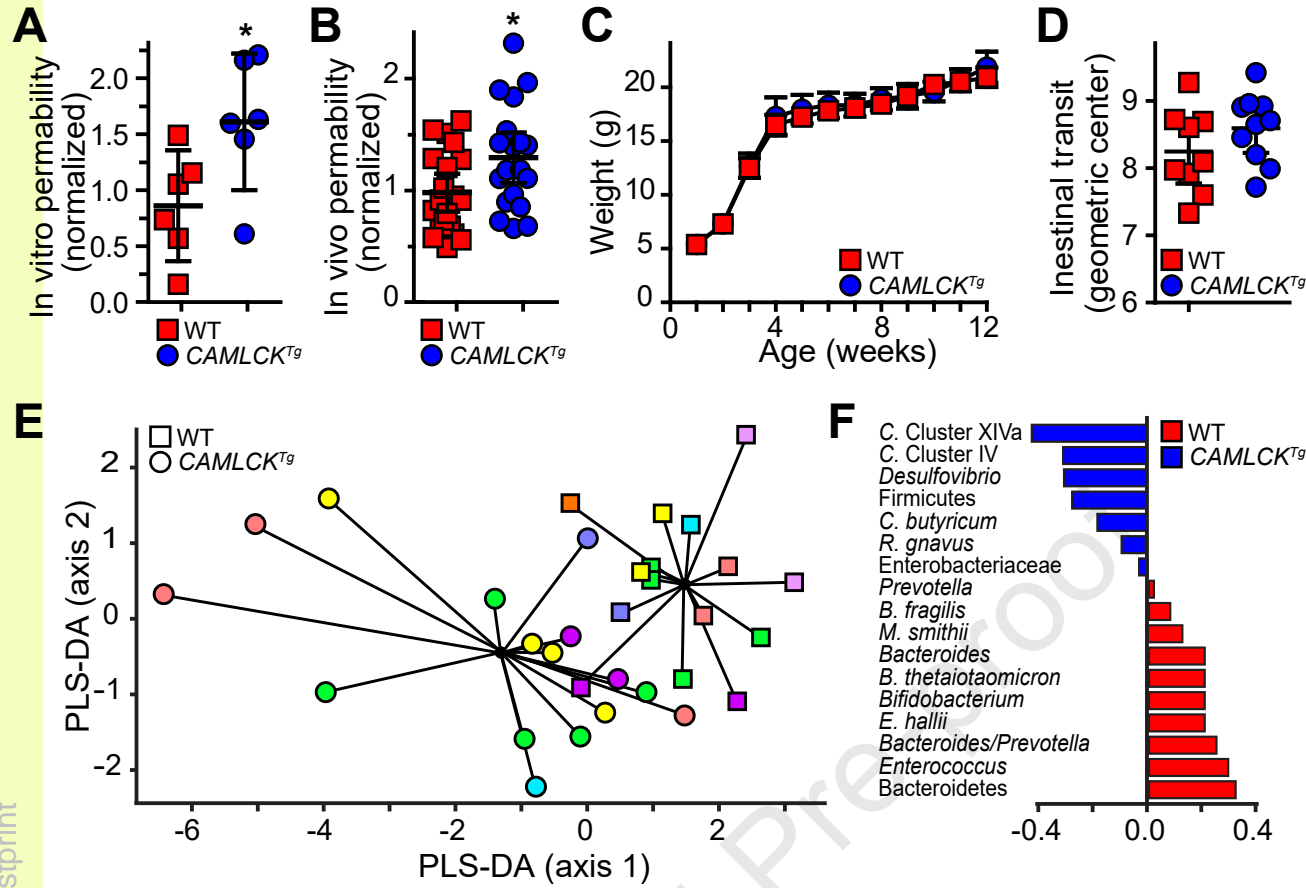
Inczeft, O., Bacquie, V., Olier Pierre, M., Rincel, M., Ringot-Destrez, B., Ellero Simatos, S., Eutamene, H., Bétoulières, C., Thomas, J., Laine, J., Gross, L., Lévêque, M., Leonard, Harkat, C., Robbe-Masselot, Roka, R., Mercier-Bonin, M., Theodorou, V., Darnaudéry, M., Turner, J. R., Ferrier, L. (Auteur de correspondance) (2020). Targeted intestinal tight junction



Journal Pre-proof

Comment citer ce document :

Inczeffi, O., Bacquié, V., Olier Pierre, M., Rincel, M., Ringot-Destrez, B., Ellero Simatos, S., Eutamene, H., Bétoulières, C., Thomas, J., Laine, J., Gross, L., Lévêque, M., Leonard, Harkat, C., Robbe-Masselot, Roka, R., Mercier-Bonin, M., Theodorou, V., Darnaudéry, M., Turner, J. R., Ferrier, L. (Auteur de correspondance) (2020). Targeted intestinal tight junction



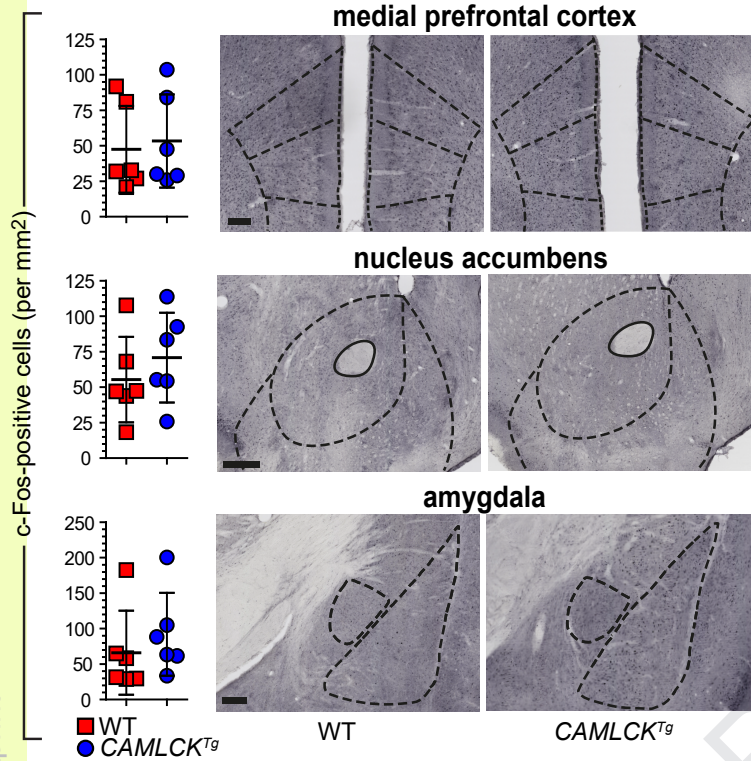
Version postprint

Journal Pre-proof

Comment citer ce document :

Inczeffi, O., Bacquié, V., Olier Pierre, M., Rincel, M., Ringot-Destrez, B., Ellero Simatos, S., Eutamene, H., Bétoulières, C., Thomas, J., Laine, J., Gross, L., Lévêque, M., Leonard, Harkat, C., Robbe-Masselot, Roka, R., Mercier-Bonin, M., Theodorou, V., Darnaudéry, M., Turner, J. R., Ferrier, L. (Auteur de correspondance) (2020). Targeted intestinal tight junction

Version postprint



Journal Pre-proof

Supplemental Figure 1:

A. Trans-jejunal fluorescein flux was increased in *CAMLCK^{Tg}* (blue circles) relative to WT (red squares) littermates. mean±SD; *, $p<0.05$, Mann-Whitney U test.

B. In vivo analysis using FITC-4kDa dextran demonstrated increased permeability of *CAMLCK^{Tg}* (blue circles, n=19) relative to WT (red squares, n=20) littermates. mean±SD; *, $p<0.05$, t-test.

C. Weight gain was similar in WT (red squares, n=6) and *CAMLCK^{Tg}* (blue circles, n=6) littermates. mean±SD.

D. Intestinal transit was similar in WT (red squares, n=10) and *CAMLCK^{Tg}* (blue circles, n=9) littermates. mean±SD.

E. Partial least squares discriminant analysis (PLS-DA) score plot based on the relative abundances of 18 microbial taxa in gut contents of *CAMLCK^{Tg}* (circles, n=16) and WT (squares, n=15) born to 8 different dams (each color represents one dam).

F. Relative abundances of microbial communities in *CAMLCK^{Tg}* (blue) and WT (red) mice. Diagrams indicate regions analyzed.

Comment citer ce document :

Inczefi, O., Bacquié, V., Olier Pierre, M., Rincel, M., Ringot-Destrez, B., Ellero Simatos, S., Eutamene, H., Bétoulières, C., Thomas, J., Laine, J., Gross, L., Lévêque, M., Leonard, Harkat, C., Robbe-Masselot, Roka, R., Mercier-Bonin, M., Theodorou, V., Darnaudéry, M., Turner, J. R., Ferrier, L. (Auteur de correspondance) (2020). Targeted intestinal tight junction

Supplemental Figure 2:

CAMLCK^{Tg} (blue circles, n=5-6) and WT (red squares, n=5-6) littermates. Representative images of C-Fos immunolabeled brains from *CAMLCK^{Tg}* and WT mice. Bars = 200µm; mean±SEM; *, $p < 0.05$, t-test.

Journal Pre-proof

Comment citer ce document :

Inczefi, O., Bacquié, V., Olier Pierre, M., Rincel, M., Ringot-Destrez, B., Ellero Simatos, S., Eutamene, H., Bétoulières, C., Thomas, J., Laine, J., Gross, L., Lévêque, M., Leonard, Harkat, C., Robbe-Masselot, Roka, R., Mercier-Bonin, M., Theodorou, V., Darnaudéry, M., Turner, J. R., Ferrier, L. (Auteur de correspondance) (2020). Targeted intestinal tight junction

Supplemental Methods

Animals

CAMLCK^{Tg} mice¹⁻⁴ (Tg(Vil-FLAG-CAMLCK)#Jrt) were maintained as male heterozygotes on C57BL/6J background. These were mated with WT C57BL/6J females to produce WT and *CAMLCK^{Tg}* littermates. At weaning, female mice were separated and housed at constant temperature (22±1°C) with a 12 hour light/dark cycle. Food (Teklad 2018, Envigo) and water were available ad libitum. All experiments were performed at 8 weeks of age. Procedures were approved by the Ethical Committee CEEA-86, under the number APAFiS#4145.

Gut microbiota composition analysis

Gut microbiota were analyzed in two cohorts (15 WT and 16 *CAMLCK^{Tg}*) from 8 different WT dams. At sacrifice, colonic contents were stored at -80°C. DNA was extracted using the ZR fecal DNA MiniPrep kit (Zymo Research) and adjusted to 1 ng/μL. Changes in relative abundance of 24 microbial 16S rRNA gene targets were obtained by qRTPCR using an adapted Gut Low-Density Array platform.⁵⁻⁷ A universal bacterial primer set was included as the reference gene. qRTPCR was performed in duplicate on a ViiA7 (Applied Biosystems).

Fluorescence data was imported into LinRegPCR to perform baseline corrections, calculate mean PCR efficiency per amplicon group. and calculate initial quantities. Among the 24 targeted amplicon groups, 6 were not detected in any fecal samples and were removed from the analysis (*B. vulgatus*, *Alistipes spp.*, *Parabacteroidetes distasonis*, *Roseburia spp.*, *E. coli* and *A. muciniphila*). Normalized N₀-values were log₁₀-transformed and processed by MixOmics (v6.1.1) with RStudio (v1.0.44) to build a partial least-squares discriminant analysis (PLS-DA). This multivariate supervised approach projects samples (X) onto a low-dimensional space of latent variables to maximize separation between groups according (Y=genotype). Leave-one-out cross-validation was used to select the optimal number of latent variables for PLS-DA models.

Open field test

Mice explored a 50x50cm arena (illumination 300lux) for 10min. Exploration was automatically assessed using a video tracking system (Bioseb). The percentage of distance traveled and time spent and in the center area (20x20cm) and total distance traveled in the entire arena were assessed.

Comment citer ce document :

Inczefi, O., Bacquié, V., Olier Pierre, M., Rincel, M., Ringot-Destrez, B., Ellero Simatos, S., Eutamene, H., Bétoulières, C., Thomas, J., Laine, J., Gross, L., Lévêque, M., Leonard, Harkat, C., Robbe-Masselot, Roka, R., Mercier-Bonin, M., Theodorou, V., Darnaudéry, M., Turner, J. R., Ferrier, L. (Auteur de correspondance) (2020). Targeted intestinal tight junction

Colorectal distension (CRD)

Two 0.08mm diameter electrodes were implanted in the abdominal external oblique muscle and a third in the abdominal skin. On postoperative days 3-6, CRD was performed using a balloon catheter (Fogarty 4F catheter, 1.1cm length, tip 3.5cm from the anus)⁸ in 10 sec periods with increasing volumes from 0.02 mL to 0.10 mL, with 5min rest between distensions. Abdominal electromyography activity was registered after the amplification (10000x) and analyzed (Powerlab Chart 5). Basal EMG activity was subtracted from EMG activity registered during distension. Some mice were treated with ML-7 (2 mg/kg i.p.) or naloxone sulfate (2 mg/kg i.p.) 1h before CRD. For others, water avoidance stress was induced on a floating platform (3cmx3cm) in the middle of a water-filled tank (40cmx40cm) for 1h daily over four days. Recovery (30min) preceded CRD.

Gastrointestinal transit

Animals received 70 μ L of 100mg/ml TRITC-70kDa dextran in tap water by gavage and were sacrificed 1 h later.⁹ Stomach, small and large intestine were cut in 11 equal parts. Luminal contents of each segment were centrifuged and fluorescence determined. Transit was calculated as the geometric center of the values for each mouse.

Ussing chamber analysis

Jejunal sections were mounted in Ussing chambers (Physiologic Instruments) filled with Krebs buffer and continuously oxygenated (95% O₂, 5% CO₂). After 1 hour of equilibration, Fluorescein (1mg/mL) was added in the apical chamber and fluorescence intensity of the basolateral chamber was measured after 1 hour.

In vivo permeability analysis

Mice were fasted for 4 hours before gavage with 150 μ L of 100mg/mL FITC-4kDa dextran in tap water. Blood (200 μ L) was collected after 4h and plasma fluorescence determined.

Comment citer ce document :

Inczefi, O., Bacquié, V., Olier Pierre, M., Rincel, M., Ringot-Destrez, B., Ellero Simatos, S., Eutamene, H., Bétoulières, C., Thomas, J., Laine, J., Gross, L., Lévêque, M., Leonard, Harkat, C., Robbe-Masselot, Roka, R., Mercier-Bonin, M., Theodorou, V., Darnaudéry, M., Turner, J. R., Ferrier, L. (Auteur de correspondance) (2020). Targeted intestinal tight junction

C-Fos analysis

Vibratome sections (40µm) were stained using polyclonal rabbit anti-C-Fos (Santa Cruz) and secondary HRP-conjugated goat anti-rabbit antisera (Jackson ImmunoResearch). NDPI images (x20) were obtained (Nanozoomer, Hamamatsu Photonics) and converted into TIFF format using ImageJ (NDPI tools plugin). Regions of interest (ROI) were manually circumscribed using ROI tools and C-Fos-immunoreactive cells quantified automatically using the particle analysis function (size: 5-20 µm²; circularity: 0.5-1). For each animal, 3-6 sections of each brain area were assessed by a blinded observer.

Statistical analysis

Statistical significance was determined by two-tailed t-test, two-tailed Mann-Whitney U test, or 2-way ANOVA and set at $p < 0.05$. For microbial analyses, univariate analysis was realized in parallel to compare each amplicon separately using unpaired t-test followed by the Benjamini-Hochberg adjustment of p -values for multiple comparisons.

Supplemental references

1. Su L, et al. *Gastroenterology* 2009;136:551-63.
2. Weber CR, et al. *J Biol Chem* 2010;285:12037-46.
3. Edelblum KL, et al. *Cell Mol Gastroenterol Hepatol* 2017;4:285-297.
4. Yu D, et al. *Proc Natl Acad Sci U S A* 2010;107:8237-41.
5. Bergstrom A, et al. *FEMS Microbiol Lett* 2012;337:38-47.
6. Bergstrom A, et al. *Appl Environ Microbiol* 2014;80:2889-900.
7. Riba A, et al. *Gastroenterology* 2017;153:1594-1606 e2.